Sensors and Materials, Vol. 35, No. 2 (2023) 491–497
MYU Tokyo

S & M 3186

Annealing Temperature Dependence of Scintillation Properties of Ga-doped ZnO Translucent Ceramics

Toshiaki Kunikata,* Takumi Kato, Daiki Shiratori, Prom Kantuptim, Daisuke Nakauchi, Noriaki Kawaguchi, and Takayuki Yanagida

Nara Institute of Science and Technology, 8916-5 Takayama, Ikoma, Nara 630-0192, Japan

(Received September 30, 2022; accepted January 11, 2023)

Keywords: Ga-doped ZnO, scintillation, translucent ceramic, annealing effect

Ga-doped ZnO translucent ceramics were prepared by spark plasma sintering and annealed at temperatures of 600, 650, 700, 750, and 800 °C for 24 h in air. The scintillation and optical properties of the non-annealed and annealed ZnO:Ga translucent ceramics were investigated. An absorption band from 550 to 800 nm was observed in the diffuse transmittance spectra of all the ZnO:Ga samples. In the scintillation spectra, all the ZnO:Ga samples exhibited defect-related emissions peaking at 500 nm under X-ray irradiation. Among the samples, the annealed ZnO:Ga translucent ceramic sample annealed at 700 °C showed the highest light yield (12000 photons/5.5 MeV-α).

1. Introduction

Some luminescent materials, such as scintillators and dosimetric materials, are used for radiation detection and dosimetry. Scintillators can convert ionizing radiation into low-energy photons[(1)] and are applied for radiation detection in fields such as environmental monitoring,[(2)] resource exploration,[(3)] astrophysics,[(4)] medical diagnoses,[(5)] and security inspections.[(6)] Dosimetric materials, including thermoluminescence, optically stimulated luminescence, and radiophotoluminescence materials,[(7)] are used as personal dosimeters. Various types of scintillators and dosimetric materials have been developed and are still being intensively studied. These materials include sintered ceramics,[(8,9)] glasses,[(10–20)] single crystals,[(21–37)] and organic materials[(38)].

Although most reported scintillators have been insulators, semiconductor materials such as CuI,[(39)] GaN,[(40)] and Ga_2O_3[(41,42)] have been considered as candidate scintillators having a high light yield (*LY*) and fast decay time. In addition, the semiconductor Ag-doped ZnS (ZnS:Ag) is an excellent scintillator with a band gap energy of 3.7 eV, an emission peak at around 450 nm, and a high *LY* (90000 photons/MeV). The scintillator ZnS:Ag is in practical use in α-particle detectors[(43–45)] owing to its high *LY* under α-particle irradiation. The disadvantage of ZnS:Ag is the difficulty of growing a transparent single crystal owing to its structural phase transition from hexagonal to cubic at 1020 °C.[(46)] Therefore, opaque ZnS:Ag ceramics prepared below 1020 °C are widely used.

*Corresponding author: e-mail: kunikata.toshiaki.kt1@ms.naist.jp
https://doi.org/10.18494/SAM4145

ISSN 0914-4935
https://myukk.org/

ZnS:Ag ceramics exhibit low energy resolution owing to their opacity. On the other hand, the semiconductor scintillator ZnO has a medium band gap (3.37 eV at 300 K), a medium density (5.6 g/cm^3), and a suitable effective atomic number (28.4) for α-particle detection. In contrast to ZnS:Ag, transparent single crystals[47] and translucent ceramics[48,49] of ZnO can be obtained. The scintillator ZnO is expected to show higher energy resolution than ZnS:Ag owing to its high transparency, and it can potentially be an alternative material to ZnS:Ag for α-particle detection. However, large ZnO single crystals are difficult to grow because ZnO single crystals are generally grown by the hydrothermal method and cannot be grown by melt-growth methods such as the Czochralski and Bridgman–Stockbarger methods owing to their low boiling point. ZnO translucent ceramics can be obtained at temperatures lower than those used in the melt-growth methods; therefore, we have been focusing on ZnO translucent ceramics as scintillators.

We previously reported the scintillation properties of non-doped ZnO translucent ceramics prepared by spark plasma sintering (SPS). The non-doped ZnO translucent ceramics were annealed at temperatures from 600 to 800 °C in steps of 50 °C in air to optimize the scintillation properties.[50] Defect-related luminescence was observed in the samples, and the highest scintillation *LY* among the non-doped ZnO translucent ceramics was 44,000 photons/5.5 MeV-α. Thus, a ZnO translucent ceramic with a high *LY* was obtained. In addition, we have recently been interested in the effect of dopants on the scintillation properties of ZnO translucent ceramics obtained by SPS. Possible dopants for ZnO include Cd,[51,52] Li,[53,54] Ag,[55] and In.[48,52,56] Ga is one of the most well-known dopants for ZnO. Although there have been many studies on the scintillation properties of Ga-doped ZnO (ZnO:Ga),[39,48,49,57–59] there have been no studies on the annealing temperature dependence of the scintillation properties of ZnO:Ga translucent ceramics prepared by SPS.

In this study, we investigated ZnO:Ga translucent ceramics with different annealing temperatures. We prepared 0.1% ZnO:Ga translucent ceramics by SPS,[20] which were annealed at different temperatures (600–800 °C in steps of 50 °C) in air. The non-annealed and annealed ZnO:Ga samples were characterized by obtaining their optical and scintillation properties. In addition, the experimental results for ZnO:Ga samples in this study are discussed and compared with those for non-doped ZnO in our previous study.[53]

2. Materials and Methods

We prepared the ZnO:Ga translucent ceramics using an SPS furnace (SinterLand LabX-100) in vacuum.[60] First, the raw material powders of ZnO (4N, Kojundo Chemical) and Ga_2O_3 (4N, Furuuchi Chemical) were mixed with 0.1 mol% Ga. The total mass of the mixed ZnO:Ga powder was adjusted to 0.5 g. Then, the ZnO:Ga powder was introduced into a cylindrical graphite die with a hole of 10.4 mm, and the die was inserted between two graphite punches. The sintering conditions were the same as those of non-doped ZnO in the previous study.[50] Two ZnO:Ga translucent ceramics were prepared under the same conditions. The surfaces of the ceramics were polished to a thickness of about 0.5 mm. Then, we cut the polished ceramics into six pieces. With an electric furnace (FT-01X, Full-Tech), the five pieces were annealed at 600, 650, 700,

750, or 800 °C for 24 h in air. The non-annealed and annealed ZnO:Ga samples were used for the characterization.

A spectrophotometer (SolidSpec-3700, Shimadzu) was used to evaluate the diffuse transmittance spectra from 300 to 800 nm. X-ray-induced scintillation spectra in the observation range of 300–690 nm were measured using our original setup.[61] The voltage and current used for X-ray irradiation to obtain the scintillation spectra were 40 kV and 1.2 mA, respectively. Pulse height spectra were measured using our original setup with a shaping time of 5 μs. In this measurement, ^{241}Am was used as the α-particle (5.5 MeV) source.[62] To estimate the scintillation *LY*, we compared the ZnO:Ga ceramics with a Ce-doped $Y_3Al_5O_{12}$ (YAG) single crystal as the reference sample, which has a scintillation *LY* of 12000 photons/5.5 MeV-α.[63]

3. Results and Discussion

The appearances of the non-annealed (as-prepared) and annealed ZnO:Ga ceramics under (a) room light and (b) 365 nm UV light are shown in Fig. 1. All samples were confirmed to be translucent. Under room light, the colors of the samples varied from dark blue to light blue depending on the annealing temperature. On the other hand, all samples showed visible luminescence under 365 nm UV illumination. The luminescence colors were changed from blue to orange by annealing. Non-uniformity of the luminescence in the samples was observed under 365 nm UV illumination.

The diffuse transmittance spectra of the samples are shown in Fig. 2. Optical absorption edges at approximately 390 nm were observed in all samples. In the as-prepared and 600 °C-annealed ZnO:Ga samples, an absorption band from 400 to 550 nm was observed, which was not observed in the other annealed ZnO:Ga samples. This absorption band may have originated from oxygen vacancies (V_O).[54] High-temperature annealing in air may reduce the V_O density. On the other hand, we observed another absorption band in the wavelength range longer than 550 nm, which was considered to be due to the absorption of free charge carriers.[48] The transmittance from 550 to 800 nm was higher in the samples annealed at higher temperatures. The mechanism of this phenomenon can be explained as follows. The generation of V_O in ZnO increases the n-type charrier density, which can increase the absorption of free charge carriers. Therefore, the absorption decreases with the decreased V_O density resulting from annealing at higher temperatures.

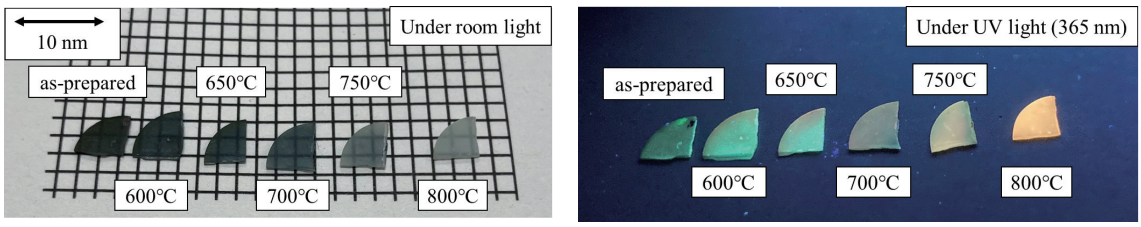

(a) (b)

Fig. 1. (Color online) Non-annealed and annealed ZnO:Ga samples under (a) room light and (b) 365 nm UV light.

Figure 3 shows X-ray-induced scintillation spectra of all the samples. Although ZnO can exhibit near-band-edge emission at around 390 nm due to free exciton recombination, none of the samples in this study had a peak at around 390 nm. This was considered to be due to the low transmittance in the short-wavelength region. In contrast, all samples showed a broad emission peak at 500 nm, which is ascribed to defect-related luminescence.[54,64,65] It has been suggested that several types of defects may contribute to this emission because the spectral shape is non-Gaussian.[54] Previous literature suggested that the scintillation peaks at around 500–600 nm are due to lattice defects such as V_O, zinc vacancies (V_{Zn}), and interstitial zincs (Zn_i). Electron transitions between energy levels such as $Zn_i \rightarrow V_{Zn}$, $V_O \rightarrow V_{Zn}$, and valence band$\rightarrow V_O$ were reported as possible origins of the luminescence.[66] Although the mechanism of the defect-related luminescence of ZnO is still unclear, V_O and V_{Zn} are considered to be strongly related. The existence ratio of these defects depends on the preparation atmosphere. For example, zinc defects and oxygen defects can be formed in oxidizing and reducing atmospheres, respectively. In addition, it has been reported that dopants sometimes affect and sometimes do not affect the spectral shape of the defect-related luminescence of ZnO. In the case of Cd-doped ZnO, the emission peak does not shift compared with that of non-doped ZnO.[51,52] It has also been reported that the peak position of In-doped ZnO (500 nm) is different from that of non-doped ZnO (550 nm).[52] We have also confirmed that the peak position of defect-related luminescence in non-doped ZnO (500–550 nm) depends on the preparation conditions.[50] Therefore, the peak position can change with the existence ratio of several defects due to impurity ion doping. In the present study, ZnO:Ga ceramics showed an emission peak at around 500 nm. This value is reasonable compared with the peak wavelength range (500–550 nm) of defect-related luminescence in non-doped ZnO ceramics.[50]

Although the samples showed different colors depending on the annealing temperature under 365 nm UV light, as shown in Fig. 1(b), all samples showed similar spectral shapes. It was considered that the difference in colors was caused by differences in the wavelength dependence of the absorption.

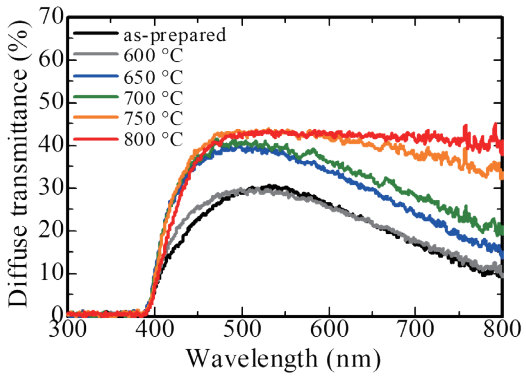

Fig. 2. (Color online) Diffuse transmittance spectra of ZnO:Ga samples.

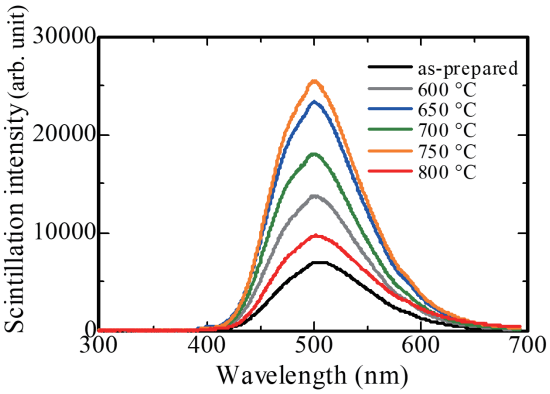

Fig. 3. (Color online) Scintillation spectra of ZnO:Ga samples under X-ray irradiation.

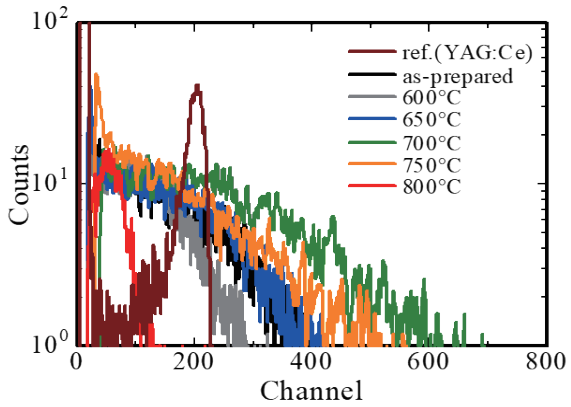

Fig. 4. (Color online) Pulse height spectra of ZnO:Ga samples and YAG:Ce reference sample under α-particle irradiation from an ^{241}Am source.

Figure 4 shows the pulse height spectra of all the samples under 5.5 MeV α-particle irradiation from ^{241}Am. No full energy absorption peaks were clearly observed in the ZnO:Ga samples due to the low energy resolution. The low energy resolution may have been caused by the nonuniformity of the luminescence intensities in the samples under UV light [Fig. 1(b)] or the insufficient diffuse transmittance as shown in the transmittance spectra (Fig. 2). Since the full energy absorption peaks were unobservable in these pulse height spectra, accurate peak fitting could not be performed. Instead of peak fitting, we assumed that the peaks are located around the positions (horizontal axes) where their pulse counts (vertical axes) begin to rapidly decrease in the direction of increasing channel number. Assuming that the full energy peaks of the as-prepared, 600, 650, 700, 750, and 800 °C annealed samples are at 150, 130, 140, 230, 170, and 60 channels in this estimation method, the *LY*s of the samples are roughly estimated to be around 8000, 7000, 7500, 12000, 9000, and 3000 photons/5.5 MeV-α, respectively. These values are higher than that of the In-doped ZnO thin film (625 photons/5.5 MeV-α);[56] however, they are lower than that of the non-doped ZnO translucent ceramic (44200 photons/5.5 MeV-α).[50]

4. Conclusions

We prepared 0.1% ZnO:Ga translucent ceramics by SPS, which were then annealed at 600, 650, 700, 750, and 800 °C for 24 h in air. In the diffuse transmittance spectra of the ceramics, we observed an absorption band from 550 to 800 nm due to the absorption of free charge carriers. In addition, we observed an absorption band in the short-wavelength range, which may have been due to V_O. These absorptions decreased in intensity at higher annealing temperatures. Thus, we confirmed that the transmittance properties of ZnO:Ga ceramics can be improved by annealing in air. The scintillation spectra of all samples showed defect-related luminescence at 500 nm. The sample annealed at 700 °C showed the highest scintillation *LY*, which was approximately 12,000 ph/5.5 MeV-α. The *LY* of the ZnO:Ga sample was lower than that of the non-doped ZnO in the previous study.

Acknowledgments

This work was supported by Grants-in-Aid for Scientific Reseach A (22H00309), Scientific Research B (22H02939, 21H03733 and 21H03736), and Exploratory Research (22K18997) from the Japan Society for the Promotion of Science. The Cooperative Research Project of the Research Center for Biomedical Engineering is also acknowledged.

References

1 T. Yanagida: Proc. Jpn. Acad. Ser. B, Phys. Biol. Sci. **94** (2018) 75.
2 K. Watanabe, T. Yanagida, and K. Fukuda: Sens. Mater. **27** (2015) 269.
3 C. L. Melcher: Nucl. Instrum. Methods Phys. Res. B **40** (1989) 1214.
4 M. Kole, M. Chauvin, Y. Fukazawa, K. Fukuda, S. Ishizu, M. Jackson, T. Kamae, N. Kawaguchi, T. Kawano, M. Kiss, E. Moretti, M. Pearce, S. Rydström, H. Takahashi, and T. Yanagida: Nucl. Instrum. Methods Phys. Res. A **770** (2015) 68.
5 Q. Liu, Y. Cheng, Y. Yang, Y. Peng, H. Li, Y. Xiong, and T. Zhu: Appl. Radiat. Isot. **163** (2020) 1092177.
6 J. Glodo, Y. Wang, R. Shawgo, C. Brecher, R. H. Hawrami, J. Tower, and K. S. Shah: Phys. Procedia **90** (2017) 285.
7 G. Okada, K. Hirasawa, T. Yanagida, and H. Nanto: Sens. Mater. **33** (2021) 2117.
8 T. Kato, D. Nakauchi, N. Kawaguchi, and T. Yanagida: Sens. Mater. **34** (2022) 653.
9 H. Kimura, T. Kato, D. Nakauchi, N. Kawaguchi, and T. Yanagida: Sens. Mater. **33** (2021) 2187.
10 N. Kawaguchi, H. Masai, M. Akatsuka, D. Nakauchi, T. Kato, and T. Yanagida: Sens. Mater. **33** (2021) 2215.
11 H. Masai, T. Ina, H. Kimura, N. Kawaguchi, and T. Yanagida: Sens. Mater. **33** (2021) 2155.
12 G. Ito, H. Kimura, D. Shiratori, D. Nakauchi, T. Kato, N. Kawaguchi, and T. Yanagida: Sens. Mater. **34** (2022) 685.
13 T. Kato, D. Shiratori, M. Iwao, H. Takase, D. Nakauchi, N. Kawaguchi, and T. Yanagida: Sens. Mater. **33** (2021) 2163.
14 H. Masai, Y. Yanagida, H. Kawamoto, Y. Koguchi, M. Koshimizu, and M. Yamawaki: Sens. Mater. **34** (2022) 699.
15 H. Kimura, T. Kato, D. Nakauchi, N. Kawaguchi, and T. Yanagida: Sens. Mater. **34** (2022) 691.
16 R. Nakamori, N. Kawano, A. Takaku, D. Onoda, Y. Takebuchi, H. Fukushima, T. Kato, K. Shinozaki, and T. Yanagida: Sens. Mater. **34** (2022) 707.
17 D. Shiratori, Y. Takebuchi, T. Kato, D. Nakauchi, N. Kawaguchi, and T. Yanagida: Sens. Mater. **34** (2022) 745.
18 K. Ichiba, Y. Takebuchi, H. Kimura, D. Shiratori, T. Kato, D. Nakauchi, N. Kawaguchi, and T. Yanagida: Sens. Mater. **34** (2022) 677.
19 H. Fukushima, D. Shiratori, D. Nakauchi, T. Kato, N. Kawaguchi, and T. Yanagida: Sens. Mater. **34** (2022) 717.
20 N. Kawaguchi, D. Nakauchi, T. Kato, Y. Futami, and T. Yanagida: Sens. Mater. **34** (2022) 725.
21 T. Yanagida, T. Kato, D. Nakauchi, and N. Kawaguchi: Sens. Mater. **34** (2022) 595.
22 D. Onoda, M. Akatsuka, N. Kawano, T. Kato, D. Nakauchi, N. Kawaguchi, and T. Yanagida: Sens. Mater. **34** (2022) 585.
23 P. Kantuptim, D. Nakauchi, T. Kato, N. Kawaguchi, and T. Yanagida: Sens. Mater. **34** (2022) 603.
24 P. Kantuptim, H. Fukushima, H. Kimura, D. Nakauchi, T. Kato, M. Koshimizu, N. Kawaguchi, and T. Yanagida: Sens. Mater. **33** (2021) 2195.
25 K. Okazaki, D. Onoda, D. Nakauchi, N. Kawano, H. Fukushima, T. Kato, N. Kawaguchi, and T. Yanagida: Sens. Mater. **34** (2022) 575.
26 M. Akatsuka, H. Kimura, D. Onoda, D. Shiratori, D. Nakauchi, T. Kato, N. Kawaguchi, and T. Yanagida: Sens. Mater. **33** (2021) 2243.
27 D. Nakauchi, T. Kato, N. Kawaguchi, and T. Yanagida: Sens. Mater. **33** (2021) 2203.
28 H. Fukushima, M. Akatsuka, H. Kimura, D. Onoda, D. Shiratori, D. Nakauchi, T. Kato, N. Kawaguchi, and T. Yanagida: Sens. Mater. **33** (2021) 2235.
29 Y. Fujimoto, D. Nakauchi, T. Yanagida, M. Koshimizu, and K. Asai: Sens. Mater. **33** (2021) 2147.
30 Y. Takebuchi, T. Kato, D. Nakauchi, N. Kawaguchi, and T. Yanagida: Sens. Mater. **34** (2022) 645.
31 M. Koshimizu, N. Kawano, A. Kimura, S. Kurashima, M. Taguchi, Y. Fujimoto, and K. Asai: Sens. Mater. **33** (2021) 2137.
32 T. Yanagida, Y. Fujimoto, K. Fukuda, and V. Chani: Nucl. Instrum. Methods Phys. Res. A **729** (2013) 58.

33 E. V. D. van Loef, P. Dorenbos, and C. W. E. van Eijk: Appl. Phys. Lett., **79**, (2001) 1573.
34 Y. Fujimoto, D. Nakauchi, T. Yanagida, M. Koshimizu, and K. Asai: Sens. Mater. **34** (2022) 629.
35 D. Nakauchi, H. Fukushima, T.: Kato, N.: Kawaguchi, and T. Yanagida: Sens. Mater. **34** (2022) 611.
36 M. Akatsuka, N. Daisuke, K. Takumi, N. Kawaguchi, and T. Yanagida: Sens. Mater. **34** (2022) 619.
37 M. Koshimizu, S. Kurashima, A. Kimura, M. Taguchi, T. Yanagida, Y. Fujimoto, and K. Asai: Sens. Mater. **34** (2022) 637.
38 A. Watanabe, A. Magi, M. Koshimizu, A. Sato, Y. Fujimoto, and K. Asai: Sens. Mater. **33** (2021) 2251.
39 S. E. Derenzo, M. J. Weber, and M. K. Klintenberg: Nucl. Instrum. Methods. Phys. Res. A **486** (2002) 214.
40 T. Yanagida, T. Kato, D. Nakauchi, G. Okada, and N. Kawaguchi: Appl. Phys. Express **14** (2021) 082006.
41 T. Yanagida, G. Okada, T. Kato, D. Nakauchi, and S. Yanagida: Appl. Phys. Express **9** (2016) 042601.
42 T. Yanagida and N. Kawaguchi: Jpn. J. Appl. Phys. **59** (2020) SCCB20.
43 S. A. McElhaney, J. A. Ramsey, M. L. Bauer, and M. M. Chiles: IEEE Trans. Nucl. Sci. **37** (1990) 868.
44 S. Yamamoto and H. Tomita: Appl. Radiat. Isot. **168** (2021) 109527.
45 Y. Morishita, S. Yamamoto, K. Izaki, J. H. Kaneko, K. Toui, Y. Tsubota, and M. Higuchi: Nucl. Instrum. Methods Phys. Res. A **764** (2014) 383.
46 K. T. Lee, B. H. Choi, J. U. Woo, J. S. Kang, J. H. Paik, B. U. Chu, and S. Nahm: J. Eur. Ceram. Soc. **38** (2018) 4237.
47 T. Yanagida, Y. Fujimoto, K. Yamanoi, M. Kano, A. Wakamiya, S. Kurosawa, and N. Sarukura: Phys. Status Solidi C **9** (2012) 2284.
48 K. A. Chernenko, E. I. Gorokhova, S. B. Eronko, A. V. Sandulenko, I. D. Venevtsev, H. Wieczorek, and P. A. Rodnyi: IEEE Trans. Nucl. Sci. **65** (2018) 2196.
49 E. I. Gorokhova, G. V. Anan'eva, V. A. Demidenko, P. A. Rodnyĭ, I. V. Khodyuk, and E. D. Bourret-Courchesne: J. Opt. Technol. **75** (2008) 741.
50 T. Kunikata, T. Kato, D. Shiratori, D. Nakauchi, N. Kawaguchi, and T. Yanagida: J. Mater. Sci.: Mater. Electron. **33** (2022) 2234.
51 T. Yanagida, Y. Fujimoto, M. Miyamoto, and H. Sekiwa: Jpn. J. Appl. Phys. **53** (2014) 02BC13.
52 K. Watanabe, M. Koshimizu, Y. Fujimoto, Y. Hayashi, H. Takizawa, T. Yanagida, and K. Asai: Radiat. Meas. **106** (2017) 146.
53 T. Kunikata, T. Kato, D. Shiratori, D. Nakauchi, N. Kawaguchi, and T. Yanagida: Sens. Mater. **34** (2022) 661.
54 P. A. Rodnyi, K. A. Chernenko, E. I. Gorokhova, S. S. Kozlovskii, V. M. Khanin, and I. V. Khodyuk: IEEE Trans. Nucl. Sci. **59** (2012) 2152.
55 T. Kunikata, T. Kato, D. Shiratori, D. Nakauchi, N. Kawaguchi, and T. Yanagida: Jpn. J. Appl. Phys. **61** (2022) 062008.
56 T. Yanagida, Y. Fujimoto, A. Yoshikawa, Y. Yokota, M. Miyamoto, H. Sekiwa, J. Kobayashi, T. Tokutake, K. Kamada, and S. Maeo: IEEE Trans. Nucl. Sci. **57** (2010) 1325.
57 E. I. Gorokhova, S. B. Eron'ko, A. M. Kul'kov, E. A. Oreshchenko, K. L. Simonova, K. A. Chernenko, I. D. Venevtsev, P. A. Rodnyĭ, K. P. Lott, and H. Wieczorek: J. Opt. Technol. **82** (2015) 837.
58 E. I. Gorokhova, S. B. Eron'ko, E. A. Oreshchenko, A. V. Sandulenko, P. A. Rodnyĭ, K. A. Chernenko, I. D. Venevtsev, A. M. Kul'kov, F. Muktepavela, and P. Boutachkov: J. Opt. Technol. **85** (2018) 729.
59 R. M. Sahani, C. Kumari, A. Pandya, and A. Dixit: Sci. Rep. **9** (2019) 11354.
60 T. Kato, N. Kawano, G. Okada, N. Kawaguchi, and T. Yanagida: Nucl. Instrum. Methods Phys. Res. B **435** (2018) 296.
61 T. Yanagida, K. Kamada, Y. Fujimoto, H. Yagi, and T. Yanagitani: Opt. Mater. **35** (2013) 2480.
62 T. Yanagida, Y. Fujimoto, M. Arai, M. Koshimizu, T. Kato, D. Nakauchi, and N. Kawaguchi: Sens. Mater. **32** (2020) 1351.
63 Y. Usui, T. Kato, N. Kawano, G. Okada, N. Kawaguchi, and T. Yanagida: J. Lumin. **200** (2018) 81.
64 P. Zhan, Z. Xie, Z. Li, W. Wang, Z. Zhang, Z. Li, G. Cheng, P. Zhang, B. Wang, and X. Cao: Appl. Phys. Lett. **102** (2013) 071914.
65 P. A. Rodnyi and I. V. Khodyuk: Opt. Spectrosc. **111** (2011) 776.
66 P. M. Ratheesh Kumar, K. P. Vijayakumar, and C. Sudha Kartha: J. Mater. Sci., **42** (2007) 2598.